Molecular Vision 2005; 11:152-62 <http://www.molvis.org/molvis/v11/a17>
Received 6 August 2004 | Accepted 23 February 2005 | Published 28 February 2005

Retinal Degeneration 12 (*rd12*): A new, spontaneously arising mouse model for human Leber congenital amaurosis (LCA)

Ji-jing Pang,[1] Bo Chang,[2] Norman L. Hawes,[2] Ronald E. Hurd,[2] Muriel T. Davisson,[2] Jie Li,[3] Syed M. Noorwez,[1] Ritu Malhotra,[1] J. Hugh McDowell,[1] Shalesh Kaushal,[1] William W. Hauswirth,[1] Steven Nusinowitz,[4] Debra A. Thompson,[5] John R. Heckenlively[5]

(The first two authors contributed equally to this publication)

Departments of [1]Ophthalmology and [3]Neuroscience, College of Medicine, University of Florida, Gainesville, FL; [2]The Jackson Laboratory, Bar Harbor, ME; [4]Jules Stein Eye Institute, Harbor-UCLA Medical Center, Torrance, CA; [5]W. K. Kellogg Eye Center, The University of Michigan, Ann Arbor, MI

Purpose: To report the phenotype and characterization of a new, naturally occurring mouse model of hereditary retinal degeneration (*rd12*).

Methods: The retinal phenotype of *rd12* mice were studied using serial indirect ophthalmoscopy, fundus photography, electroretinography (ERG), genetic analysis including linkage studies and gene identification, immunohistochemistry, and biochemical analysis.

Results: Mice homozygous for the *rd12* mutation showed small punctate white spots on fundus examination at 5 months of age. The retina in the *rd12* homozygote had a normal appearance at the light microscopic level until 6 weeks of age when occasional voids appeared in the outer segments (OS) of the photoreceptor (PR) cells. The outer nuclear layer (ONL) appeared normal until 3 months of age though more obvious voids were detected in the OS. By 7 months of age, 6 to 8 layers of ONL remained in the mutant retina, and the OS were obviously shorter. The first sign of retinal degeneration was detected at the electron microscopic level around 3 weeks of age when occasional small lipid-like droplets were detected in the retinal pigment epithelium (RPE). By 3 months of age, much larger, lipid-like droplets accumulated in RPE cells accompanied by some OS degeneration. While the histology indicated a relatively slow retinal degeneration in the *rd12* homozygous mutant mice, the rod ERG response was profoundly diminished even at 3 weeks of age. Genetic analysis showed that *rd12* was an autosomal recessive mutation and mapped to mouse chromosome 3 closely linked to *D3Mit19*, a location known to be near the mouse *Rpe65* gene. Sequence analysis showed that the mouse retinal degeneration is caused by a nonsense mutation in exon 3 of the *Rpe65* gene, and the gene symbol for the *rd12* mutation has been updated to $Rpe65^{rd12}$ to reflect this. No RPE65 expression, 11-cis retinal, or rhodopsin could be detected in retinas from *rd12* homozygotes, while retinyl esters were found to accumulate in the retinal pigment epithelium (RPE).

Conclusions: Mutations in the retinal pigment epithelium gene encoding RPE65 cause an early onset autosomal recessive form of human retinitis pigmentosa, known as Leber congenital amaurosis (LCA), which results in blindness or severely impaired vision in children. A naturally arising mouse *Rpe65* mutation provides a good model for studying the pathology of human *RPE65* mutations and the effects of retinyl ester accumulation.

Leber congenital amaurosis (LCA) is the designation for a group of autosomal recessive blinding retinal dystrophies that represent the most common genetic causes of congenital visual impairment in infants and children. About 10% of LCA cases are caused by mutations in the gene encoding RPE65 [1,2]. RPE65 is a highly conserved 61 kDa protein that is present in the smooth endoplasmic reticulum of the retinal pigment epithelium (RPE) [3], and is essential for the conversion of vitamin A from all-*trans* retinol to 11-*cis* retinal, the chromophore of the visual pigments [4]. The *Rpe65* gene has been mapped in the mouse to chromosome 3 (Chr 3) in an interspecific backcross [5]. The *Rpe65* gene consists of 14 exons encoding a 533 amino acid protein [6]. To date, RPE65 studies in mouse have relied heavily on a knockout mouse reported by Redmond et al. [7]. $Rpe65^{-/-}$ mice develop a slow retinal degeneration accompanied by over accumulation of all-*trans*-retinyl esters in the RPE, while 11-*cis*-retinyl esters and 11-*cis* retinal are absent. Concomitantly, outer segment discs of rod photoreceptors in $Rpe65^{-/-}$ mice become disorganized compared with those of $Rpe65^{+/+}$ and $Rpe65^{+/-}$ mice. $Rpe65^{-/-}$ mice have severely depressed light and dark adapted electroretinogram (ERG) responses as a result of low levels of chromophore [7,8]. Residual responses are attributed to rod function having decreased sensitivity (similar to that of cones) [9] and proposed to be sustained by small amounts of 9-*cis* retinal that serves as the chromophore for opsin [10]. The associated pathogenic mechanism likely is due to increased levels of unregenerated opsin apoprotein that result in constitutive activation of the visual cascade [11].

Correspondence to: Bo Chang, MD, The Jackson Laboratory, 600 Main Street, Bar Harbor, ME 04609; Phone: (207) 288-6394; FAX: (207) 288-6149; email: bchang@jax.org

Mouse models of spontaneous retinal degenerations have been used for many years to provide insight into the etiologies of human retinal degenerations and to provide retinal tissue to study the pathology of disease progression. Mouse models of retinal degeneration have provided good initial templates for gene and pharmacological therapies. Many of these models have come from screening mice from genetically independent mouse strains and stocks at The Jackson Laboratory (TJL) by indirect ophthalmoscopy and electroretinography (ERG) [12-16]. In the present study, we have identified a new retinal degeneration mutation, retinal degeneration 12 (*rd12*), which is associated with distinctive white dots on the retina that develop with age. We show that the *rd12* retinal degeneration is caused by a nonsense mutation in exon 3 of the *Rpe65* gene. Our functional and biochemical studies confirm that vitamin A metabolism and visual processing are disrupted in the *rd12* mouse. This naturally occurring mutation (*Rpe65*^{rd12}) provides another valuable mouse model for LCA.

METHODS

Animals: The mice in this study were bred and maintained in standardized conditions in the Research Animal Facility at TJL and the University of Florida. They were maintained on NIH31 6% fat chow and acidified water, with a 14 h light/10 h dark cycle in conventional facilities that were monitored regularly to maintain a pathogen free environment. All experiments were approved by the Institutional Animal Care and Use Committees and conducted in accordance with the ARVO Statement for the Use of Animals in Ophthalmic and Vision Research.

Origin: rd12 was discovered in one male mouse of the B6.A-*H2-T18*^{a}/BoyEg strain at 10 months of age; at that time small, discrete white dots were present throughout the fundus (Figure 1). This male mouse was mated to a C57BL/6J female and then mated to the F1 female mice. The F1 mice had normal retinas, but some of the backcrossed mice showed a similar retinal phenotype with small, discrete dots in the fundus. These affected mice were mated with each other to produce the *rd12* mouse colony. Subsequently, the *rd12* stock was maintained by repeated backcrossing to C57BL/6J to make a congenic inbred strain, hereafter referred to as B6-*rd12*.

Clinical retinal evaluation: Twenty mice used in clinical characterization studies had pupils dilated with 1% atropine ophthalmic eye drops and were evaluated by indirect ophthalmoscopy with a 78 D lens. Signs of retinal degeneration, such as vessel attenuation, alterations in the RPE, and presence or absence of retinal dots were noted. Fundus photographs were taken with a Kowa Genesis small animal fundus camera (Torrance, CA) [17].

Electroretinography: After at least 6 h of dark adaptation, mice were anesthetized with an intraperitoneal injection of normal saline solution containing ketamine (15 mg/g) and xylazine (7 mg/g body weight). Electroretinograms (ERGs) were recorded from the corneal surface of one eye after pupil dilation (1% atropine sulfate) using a gold loop electrode referenced to a gold wire in the mouth. A needle electrode placed in the tail served as ground. A drop of methylcellulose (2.5%) was placed on the corneal surface to ensure electrical contact and to maintain corneal integrity. Body temperature was maintained at a constant temperature of 38 °C using a heated water pad. All stimuli were presented in a Ganzfeld dome (LKC Technologies, Gaithersburg, MD) whose interior surface was painted with a highly reflective white matte paint (No. 6080; Eastman Kodak, Rochester, NY). Stimuli were generated with a Grass Photic Stimulator (model PS33 Plus; Grass Instruments, Worcester, MA) affixed to the outside of the dome at 90° to the viewing porthole. Dark adapted responses were recorded to short wavelength (λ_{max} = 470 nm; Wratten 47A filter) flashes of light over a 4.0 log unit range of intensities (0.3 log unit steps) up to the maximum allowable by the photic stimulator. Light adapted responses were obtained with white flashes (0.3 steps) on the rod saturating background after 10 min of exposure to the background light to allow complete light adaptation. Responses were amplified (Grass CP511 AC amplifier, x10,000; 3 dB down at 2 and 10,000 Hz) and digitized using an I/O board (model PCI-1200; National Instruments, Austin, TX) in a personal computer. Signal processing was performed with custom software (LabWindows/CVI; National Instruments). Signals were sampled every 0.8 ms over a response window of 200 ms. For each stimulus condition, responses were computer averaged with up to 50 records averaged for the weakest signals. A signal rejection window could be adjusted during data collection to eliminate electrical artifacts.

Gene mapping and sequencing: To determine the chromosomal location of the *rd12* gene, we mated B6-*rd12* mice to CAST/EiJ mice. The F1 mice, which exhibit no retinal abnormalities, were backcrossed (BC) to B6-*rd12* mice. Tail DNA was isolated as previously reported [18]. DNAs of the 92 BC offspring were genotyped using microsatellite markers to develop a structure map of the region. For PCR amplification, 25 ng DNA was used in a 10 μl volume containing 50 mM KCl, 10 mM Tris-HCl, pH 8.3, 2.5 mM $MgCl_2$, 0.2 mM oligonucleotides, 200 μM dNTPs, and 0.02 U AmpliTaq DNA polymerase. The reactions, were initially denatured for 3 min at 94 °C, then subjected to 40 cycles of 15 s at 94 °C, 1 min at 51 °C, 1 min at 72 °C, and then a final 7 min extension at 72 °C. PCR products were separated by electrophoresis on 3%

Table 1. PCR primers

Gene	Primer
Rpe65-1	F: TAAGAACTTGCTTCCTCATC
	R: CTGCTTAATTGTCTCCAAGG
Rpe65-2	F: TGTAAATATCTACCCAGTGG
	R: ACATATCTCCTGACTTCAGG
Rpe65-3	F: GGTCTGACTCCCAACTATATCG
	R: TTCCAGAGCATCTGGTTGAG
Rpe65-4	F: CTAAAGAAATCTGGATGTGG
	R: oligo(dT) primer

The table lists the primers used to amplify overlapping cDNA fragments and sequence directly.

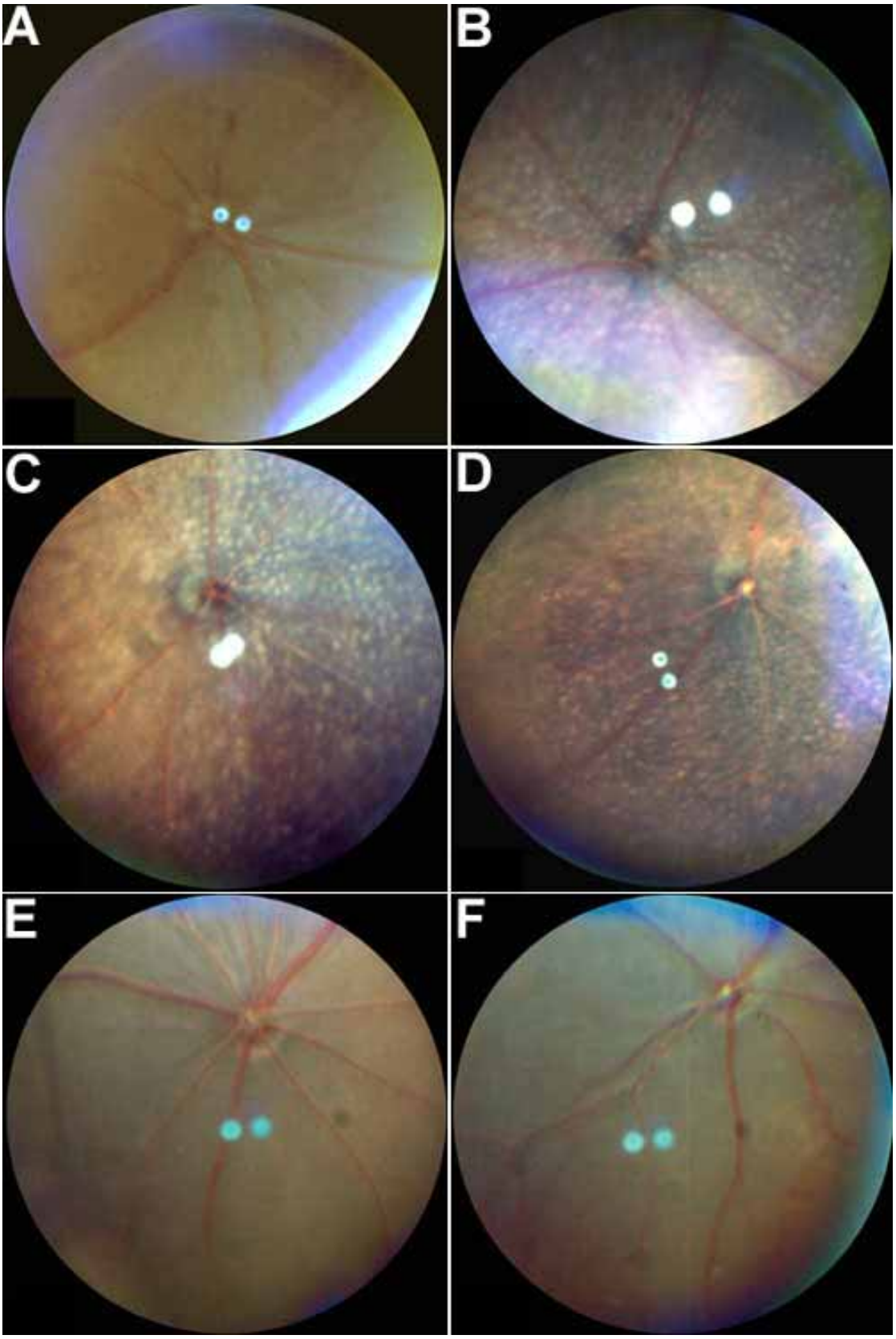

Figure 1. Fundus pictures of *rd12* homozygotes and normal C57BL/6J mice. There was no apparent fundus change in 3 month old *rd12* homozygotes (**A**) by ophthalmoscopic examination. Small, evenly spaced white dots throughout the retina became apparent by 5 months of age (**B**). These dots were still detectable in 7 month old (**C**) and 15 month old (**D**) *rd12* mice. No similar dots could be detected in fundi of C57BL/6J mice at 3 months (**E**) or 15 months (**F**).

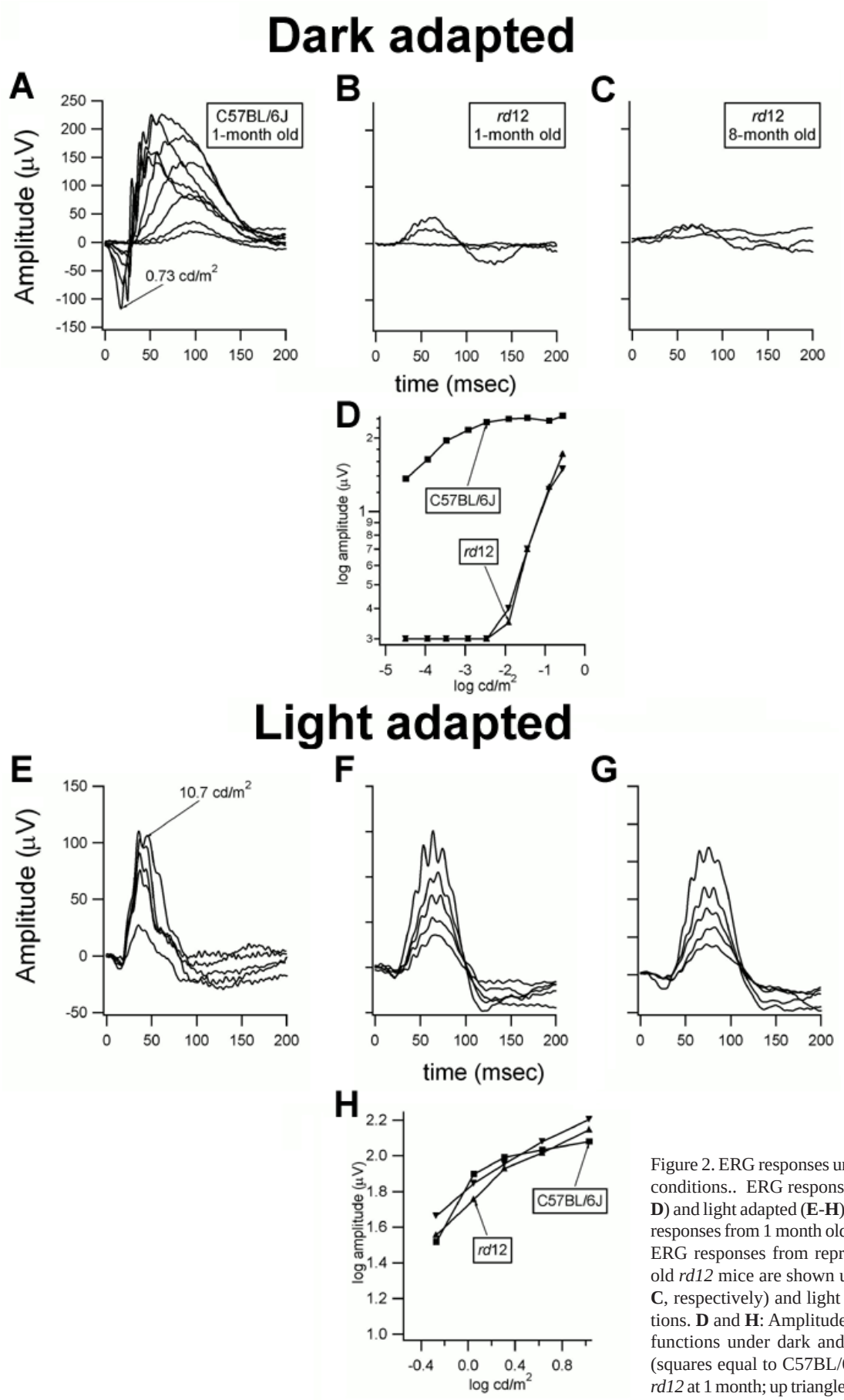

Figure 2. ERG responses under dark and light adapted conditions.. ERG responses under dark adapted (**A**-**D**) and light adapted (**E**-**H**) conditions. **A** and **E**: ERG responses from 1 month old C57BL/6J control mouse. ERG responses from representative 1 and 8 month old *rd12* mice are shown under dark adapted (**B** and **C**, respectively) and light adapted (**F** and **G**) conditions. **D** and **H**: Amplitude versus intensity response functions under dark and light adapted conditions (squares equal to C57BL/6J; down triangle equal to *rd12* at 1 month; up triangle equal to *rd12* at 8 months).

MetaPhor (FMC, Rockland, ME) agarose gels and visualized under UV light after staining with ethidium bromide. Initially a genome scan of microsatellite (Mit) DNA markers was carried out on pooled DNA samples [19]. After detection of linkage on Chromosome 3, the microsatellite markers *D3Mit19, D3Mit15, D3Mit11* were scored on individual DNA samples. To test the *Rpe65* gene as a candidate, we designed four pairs of PCR primers based on mouse coding sequence from Celera mouse genomic sequence (Celera, Foster City, CA; Biosystems) to amplify overlapping cDNA fragments. The human *RPE65* mRNA (NM_000329) sequence was used to blast the Celera mouse genome sequences. For direct sequencing, the PCR reaction was scaled up to 30 µl; amplification was done for 36 cycles with a 15 s denaturing step at 94 °C, a 2 min annealing step at 60 °C, and a 2 min extension step at 72 °C. PCR products were purified from agarose gels using a Qiagen kit (Qiagen Inc., Valencia, CA). Sequencing reactions were carried out with automated fluorescence tag sequencing. Total RNA was isolated from retinas of newborn mice by TRIZOL LS Reagent (Invitrogen life technologies, Carlsbad, CA) and the SuperScript™ preamplification system (Invitrogen life technologies) was used to make first strand cDNA. Primers used in the study are shown in Table 1.

Light and transmission electron microscopy (TEM): Both eyes from *rd12* mutant mice and age matched C57BL/6J mice were enucleated and eyecups were prepared for light and electron microscopic examination with previously described procedures [20,21]. 2-6 eyes were used for each age group. Eyes were immediately removed and immersed in cold fixative, 4% glutaraldehyde in 0.1 M phosphate buffer. Corneas were removed and the eyes left in fixative for 24 h. The lens was then removed followed by dehydration with a graded series of increasing ethanol concentrations. Eyecups were embedded in Epon mixture. For each sample, 0.5 µm thin sections were

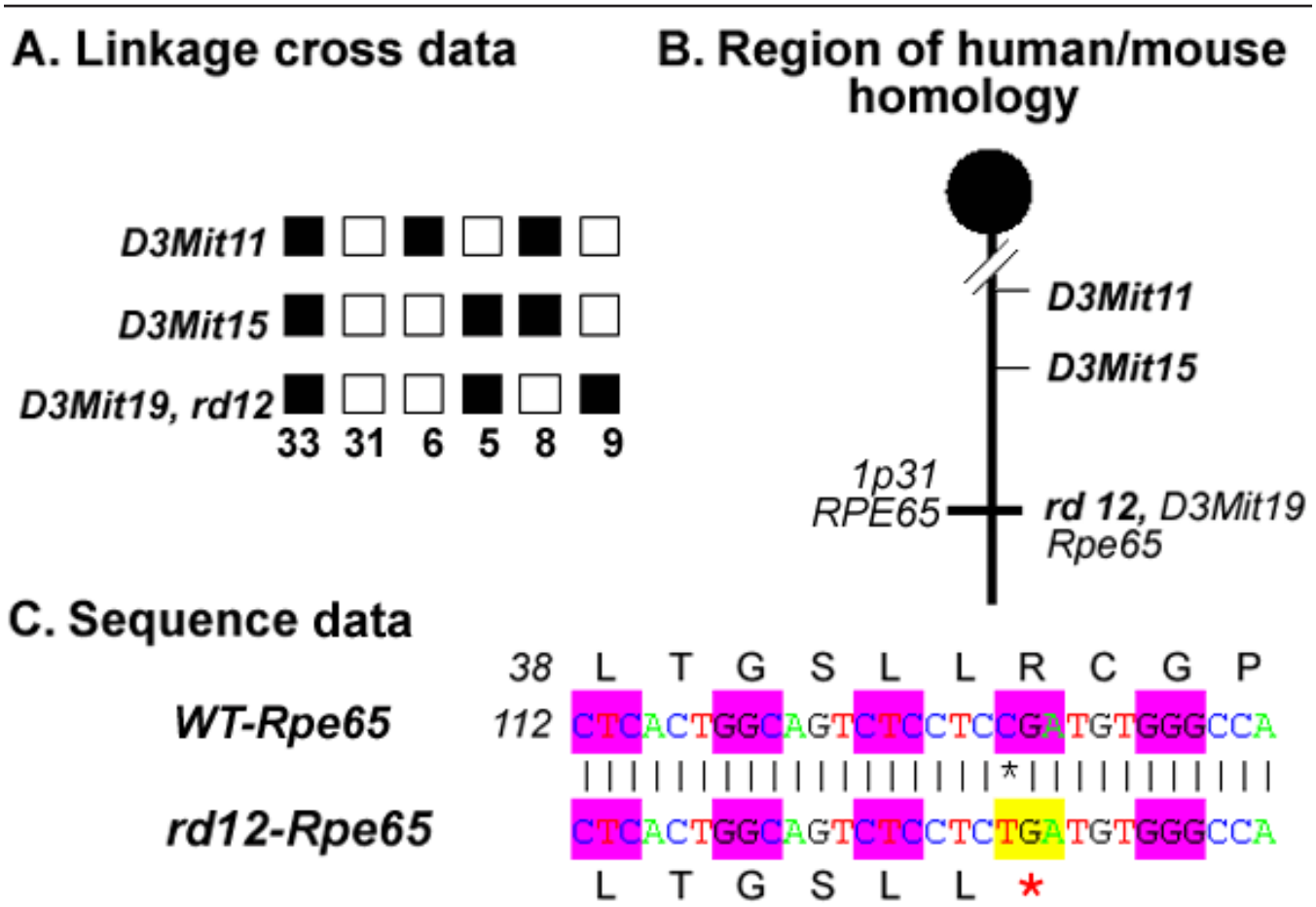

Figure 3. Linkage and sequence data. **A**: Ninety-two back-cross progeny from the (B6-*rd12* X CAST/EiJ)F1 X B6-*rd12/rd12* were phenotyped for ERG phenotype and genotyped for the indicated microsatellite markers. The black boxes represent homozygosity for B6 derived allele and white boxes represent heterozygosity, B6 and CAST derived alleles. The number of chromosomes sharing the corresponding haplotype is indicated below each column of squares. The order of marker loci was determined by minimizing the number of crossovers. The genotype for *rd12* was inferred from the phenotype. *rd12* and *D3Mit19* are tightly linked with no crossover (0/92). **B**: Genetic map of Chromosome 3 in the *rd12* region showing the closest markers (*D3Mit19* at position 87.60 cM), the retinal expressed gene *Rpe65* and the region of human homology (1p31). **C**: The nucleotide sequences around the single base substitution at position 130 (C to T) in exon 3 are shown for the wild type (WT) allele and the *rd12* allele of the *Rpe65* gene (GenBank accession number: AF410461). A novel mutation changes codon 44 CGA to a stop codon TGA (amino acid change: Arg44Ter) in the *Rpe65* gene in *rd12* mice.

stained with toluidine blue for light microscopy followed by ultra thin section preparation for TEM examination.

Immunocytochemistry for Rpe65 *expression:* Three eyes from C57BL/6J and 3 eyes from *rd12* homozygotes at 2 month of age were fixed with 4% paraformaldehyde. Eyecups were prepared as described above, and frozen with Tissue Freezing Medium (Triangle Biomedical Sciences, Durham, NC). Following permeabilization with 0.1% Triton X-100, 10 μm frozen sections were rinsed in 0.1 M PBS, blocked in 20% normal goat serum (NGS), then incubated overnight at 4 °C in rabbit polyclonal raised anti-human/bovine RPE65 antibodies (kindly provided by Dr. T. Michael Redmond, NEI, NIH), which were diluted in NGS to 1:400. After 3 rinses with 0.1 M PBS, sections were incubated in goat anti-rabbit Texas red (1:300, Molecular Probes, Eugene, OR) for 2 h followed by 3 rinses with 0.1 M PBS. Sections were then mounted with coverslips before fluorescence photography.

Purification of rhodopsin: Normal C57BL/6J and *rd12* homozygotes were dark adapted overnight, euthanized, and the eyecups were prepared by removing the cornea and lens under dim red light for each experiment. Four eyes from different mice were used for each age. Retinas were then separated from the eyecups and collected individually in 1.0 ml buffer A (10 mM sodium phosphate buffer, 137 mM NaCl, 1.0% n-Dodecyl-β-D-maltopyranoside [DM] and complete protease inhibitor cocktail [Roche Diagnostics Corporation Indianapolis, IN], pH 7.0) and sonicated for 10 s. The samples were agitated gently overnight at 4 °C in the dark. The rhodopsin was purified essentially as described by Noorwez et al. [22]. Briefly, the tubes were centrifuged at 36,000 rpm for 15 min at 4 °C in a Beckman tabletop ultracentrifuge and the supernatants collected and incubated with 1D4 coupled Sepharose 4B beads (by coupling 1D4 to CNBr activated sepharose beads from Pharmacia according to their instructions) for 3.5 h at 4 °C. The beads were washed with buffer B (10 mM sodium phosphate buffer, 0.1% DM, and complete protease inhibitor cocktail, pH 6.0) and rhodopsin eluted in buffer B containing 0.1 mM synthetic peptide corresponding to the C-terminal 18 amino acids of rhodopsin for 1 h. The tubes were spun briefly, the supernatants collected. The UV/visible spectra were recorded with a Tidas II spectrophotometer (World Precision Instruments, Sarasota, FL).

Retinoid analysis: All procedures were carried out under dim red light (>660 nm). Retinoids were analyzed following slight modifications of the procedures of Groenendijk and Smith [23,24]. Freshly purified rhodopsin from mouse retina was dried under a stream of nitrogen at room temperature. A 1:1 mixture of methanol and 1 M NH_2OH (pH 6.5), 0.1 ml, was added to each sample and the samples were mixed on a vortex shaker. Methanol was added to 70% and the samples were mixed again in a 1.7 ml centrifuge tube. Water and dichloromethane were added to yield 1:1:1 ratio of water:methanol:dichloromethane. The extracts were vortexed, briefly centrifuged, and the lower organic phase collected. Addition of dichloromethane, vortexing, centrifugation and collection of lower phase was repeated twice. The collected organic phases were combined, and dried under a stream of nitrogen gas. Samples were stored in the dark at -80 °C if not analysed immediately. The residue was dissolved in 25 μl of 1% isopropyl alcohol in hexane and an aliquot was immediately injected onto an HPLC column (Luna, 5μ Silica (2) from Phenomenex Torrance, CA) and resolved according to the pro-

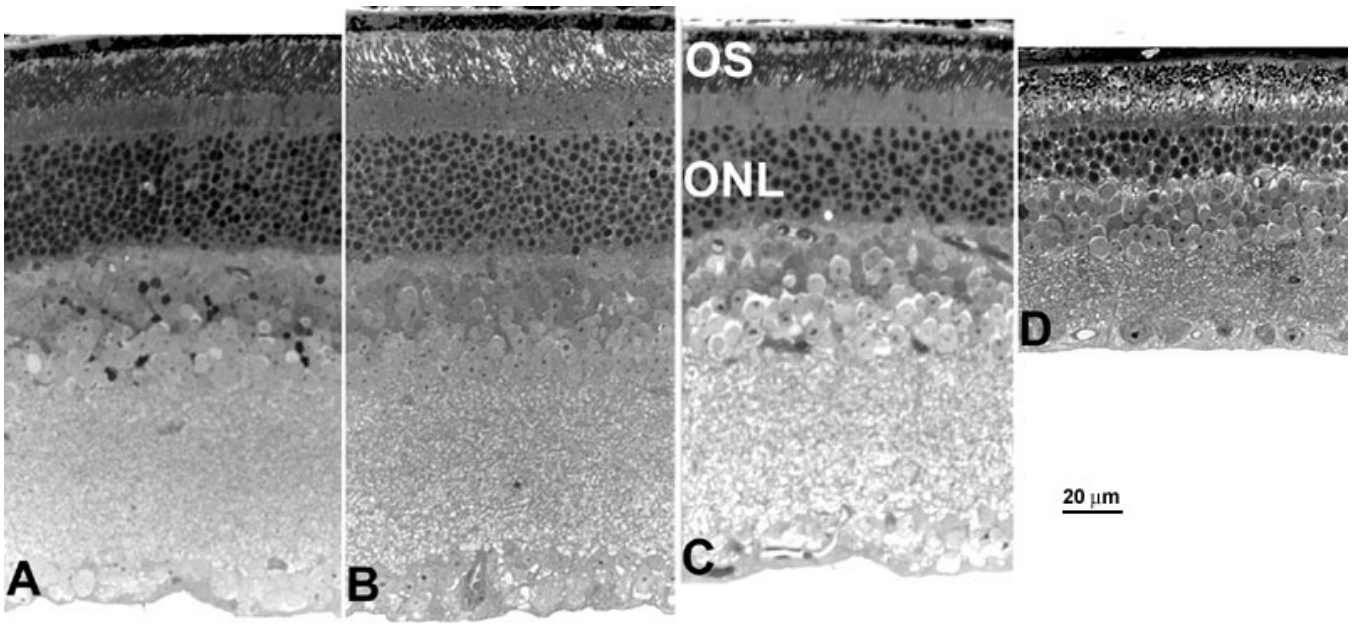

Figure 4. Light microscopic changes in *rd12* retinas at various ages. Retinas appeared normal at 6 weeks of age except some occasional outer segments (OS) voids (**A**). The thickness of the OS and outer nuclear layer (ONL) remained nearly normal at 3 months although OS were more disorganized and exhibited more voids (**B**). By 7 months, only 6 to 7 rows of ONL nuclei remained (**C**). By 27 months, most of the OS disappeared or were greatly shortened and only 3-4 layers of ONL nuclei remained (**D**). The scale bar represents 20 μm.

cedure of Smith and Goldsmith [24] using an isocratic elution with 9% ethyl acetate in hexane.

Retinyl ester quantification and analysis: At least 3 animals (6 eyes) were used for analysis at each age. From each mouse the two eyecups with their RPE cell layer intact were homogenized in 200 µl PBS. The homogenate was then extracted with 300 µl cold methanol and 300 µl hexane or 300 µl of dichloromethane and centrifuged at 10,000 x g for 5 min. The organic phase was collected and the aqueous phase was extracted twice more. The organic phase was dried under a stream of nitrogen, dissolved in 25 µl of 1% isopropyl alcohol and typically 20 µl was used to analyze for retinyl ester content by HPLC. The analysis was performed using a Luna, 5µ Silica (2) HPLC column from Phenomenex. The analysis was performed as described by Maeda et al. [25] with slight modifications to the conditions focusing on the retinyl ester elution region. After injection, the column was eluted with 1% ethyl acetate in hexane for 15 min. The column was then washed with 8% ethyl acetate in hexane for at least 5 min and then equilibrated with 1% ethyl acetate in hexane for at least 5 min.

RESULTS

Clinical phenotype: Mice homozygous for *rd12* showed small evenly spaced white dots throughout their retinas (Figure 1). These small white dots became apparent upon ophthalmoscopic examination by 5 months of age. They are under retinal vessels (that is, vessels pass over the white dots). The fundus developed a mildly pigmented granular and mottled appearance by 15 months of age; individual spots could still be seen, although less frequently, in mice up to about 2 years of age (data not shown).

ERG phenotype: ERG records obtained from *rd12* mice at 1 and 8 months of age are shown in Figure 2. Recordings obtained from a 1 month old C57BL/6J mouse are shown for comparison. Under dark adapted conditions, homozygous *rd12* mice exhibited recordable, but severely attenuated, ERG signals to the brightest stimuli, even at the earliest age tested (Figure 2B). A comparison of response amplitudes at 1 and 8 months of age relative to a normal control mouse is shown in Figure 2D. Under light adapted conditions, ERG responses were significantly more robust, with response amplitudes at or near the normal range (Figure 2H). However, the timing of peak components was delayed with respect to normal at all ages with progressive delays and amplitude loss with age (data not shown).

Genetic analysis: Genetic analysis showed that *rd12* is an autosomal recessive mutation that maps to mouse Chromosome 3. It is closely linked to *D3Mit19* (no crossover was found between *rd12* and *D3Mit19* in 92 linkage samples), suggesting that the human homolog might be on Chromosome 1p31 where the human *RPE65* gene is located (Figure 3A,B). Sequence analysis of *Rpe65* cDNA from *rd12* homozygotes showed a single base substitution at position 130 (C to T) in exon 3, which leads to a stop codon at amino acid position 44

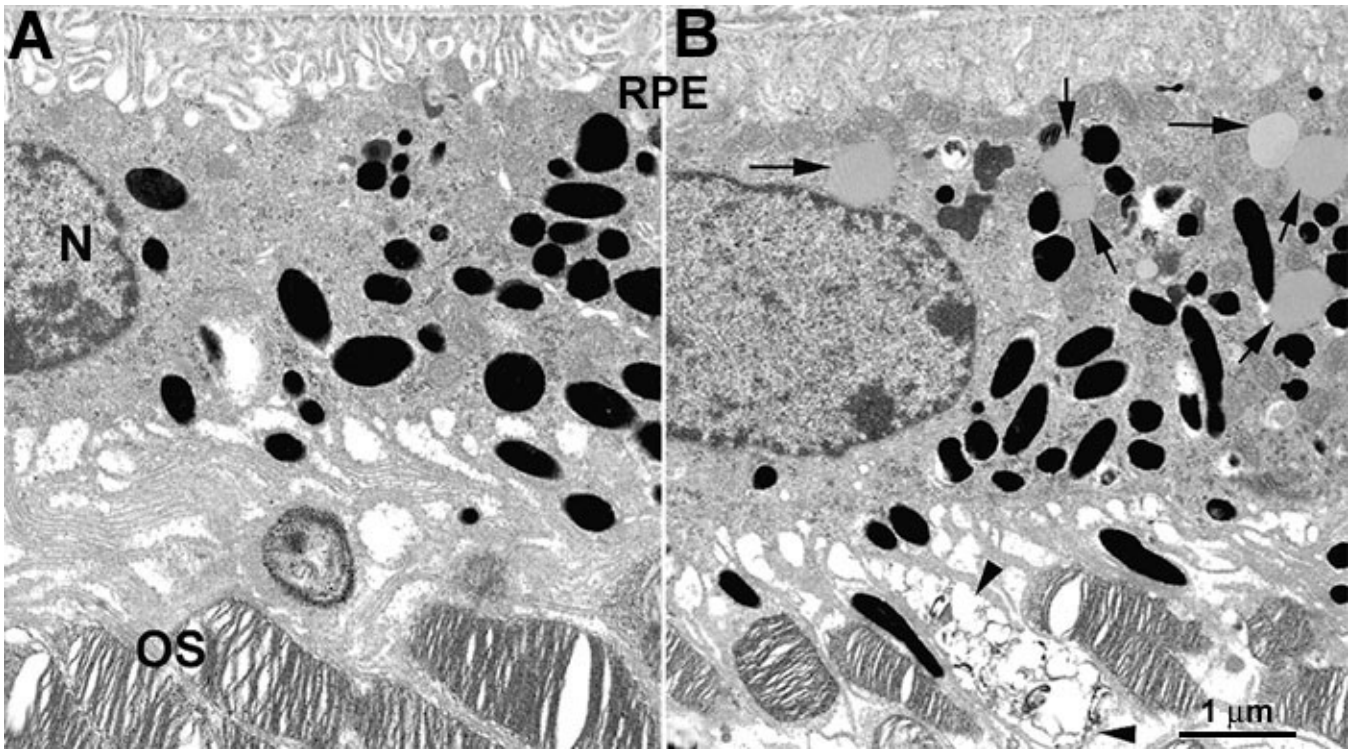

Figure 5. Electron microscopic changes in 3 month old retinas from normal C57BL/6J and *rd12* mice. **A**: Normal RPE cells. **B**: *rd12* RPE cells. No lipid-like droplets could be detected in normal RPE cells, while many typical lipid-like droplets (arrows) could be observed in the cytoplasm of *rd12* RPE cells. Degenerating outer segments (OS; arrowheads) could be observed at this age. A nucleus (N) and the retinal pigment epithelium (RPE) are also labeled. The scale bar represents 1 µm.

(CGA to TGA, Figure 3C). This single base substitution was confirmed by sequencing four more *rd12* homozygotes. There were no other changes in the *Rpe65* gene sequence compared to C57BL/6J (wildtype). We have deposited the C57BL/6J cDNA sequence of the *Rpe65* gene in GenBank (AF410461). Since the retinal degeneration in *rd12* homozygotes was caused by a nonsense mutation in exon 3 of the *Rpe65* gene, the gene symbol for the *rd12* mutation has been changed to *Rpe65*^{rd12}.

Morphological phenotype: By light microscopy, there was little change in photoreceptor cells at 6 weeks except occasional voids in the rod outer segments (OS) of *rd12* homozygotes (Figure 4A). Such voids increased progressively in frequency and size and became very obvious by 3 months of age (Figure 4B). However, the thicknesses of the OS layer and the outer nuclear layer (ONL) were maintained (Figure 4B). By 7 months of age (Figure 4C), both OS and ONL became shortened. The ONL in *rd12* homozygotes at 7 months contained 6 to 7 layers of nuclei compared with 10 to 11 layers in normal C57BL/6J mice. By 27 months (Figure 4D), the OS of rods were nearly absent while the ONL was decreased to 3-4 layers in *rd12* homozygotes. RPE cells at this age became atrophied and hypopigmented.

By TEM, RPE cells appeared normal except occasional small atypical lipid-like droplets at the age of 3 weeks in *rd12* homozygotes (data not shown). The frequency and size of lipid-like droplets increased slowly with age. By 3 months, relative to the normal C57BL/6J mice (Figure 5A), there was significant accumulation of such droplets in the RPE cytoplasm of *rd12*, with more degenerating OS, perhaps corresponding to OS voids in light microscopic picture at the same age (Figure 5B). Lipid-like droplets became progressively more frequent and larger in RPE cells with an accompanying OS shortening with age (data not shown). In contrast, there were no comparable droplets detected at any age in the RPE of C57BL/6J mice.

Biochemical phenotype: Studies of RPE65 expression using immunohistochemical analysis of retinal sections with an anti-RPE65 antibody showed that RPE65 protein was mainly localized to RPE cells in C57BL/6J mice, but was undetectable in *rd12* homozygotes (Figure 6). Quantitation of rhodopsin visual pigment, formed when opsin apoprotein combines with the chromophore 11-*cis* retinal, showed the typical UV/visible spectrum with an absorption maximum at 500 nm in C57BL/6J mice. The absorption spectra from different experiments varied by less than 5%. A representative spectrum is shown in Figure 7. No rhodopsin absorbance was detected in *rd12* homozygotes at a variety of ages from 2 weeks to 5 months, while rhodopsin had reached nearly its adult level by 5 weeks in normal C57BL/6J retina (Figure 7). In addition, the typical purified opsin protein peak at 280 nm, detectable in C57BL/6J mouse retinas as early as 8 days after birth (data not shown), was much lower in *rd12* homozygotes (Figure 7). This lower level of opsin expression in *rd12* homozygotes was confirmed by western blot analysis (data not shown). Levels of 11-*cis* retinal extracted from purified rhodopsin preparations and quantitated by HPLC analysis were undectable in the retinas of *rd12* homozygotes (data not shown). Levels of retinyl esters in normal C57BL/6J and *rd12* mice could be detected at about 3 weeks of age. In normal C57BL/6J mice, the levels remained low and stable thereafter (Figure 8). In contrast, retinyl esters in *rd12* homozygotes were detected at levels similar to normal at 3 weeks of age but increased dramatically with increasing age. While the analyses were quite variable, from 6 weeks of age there was a clear over accumu-

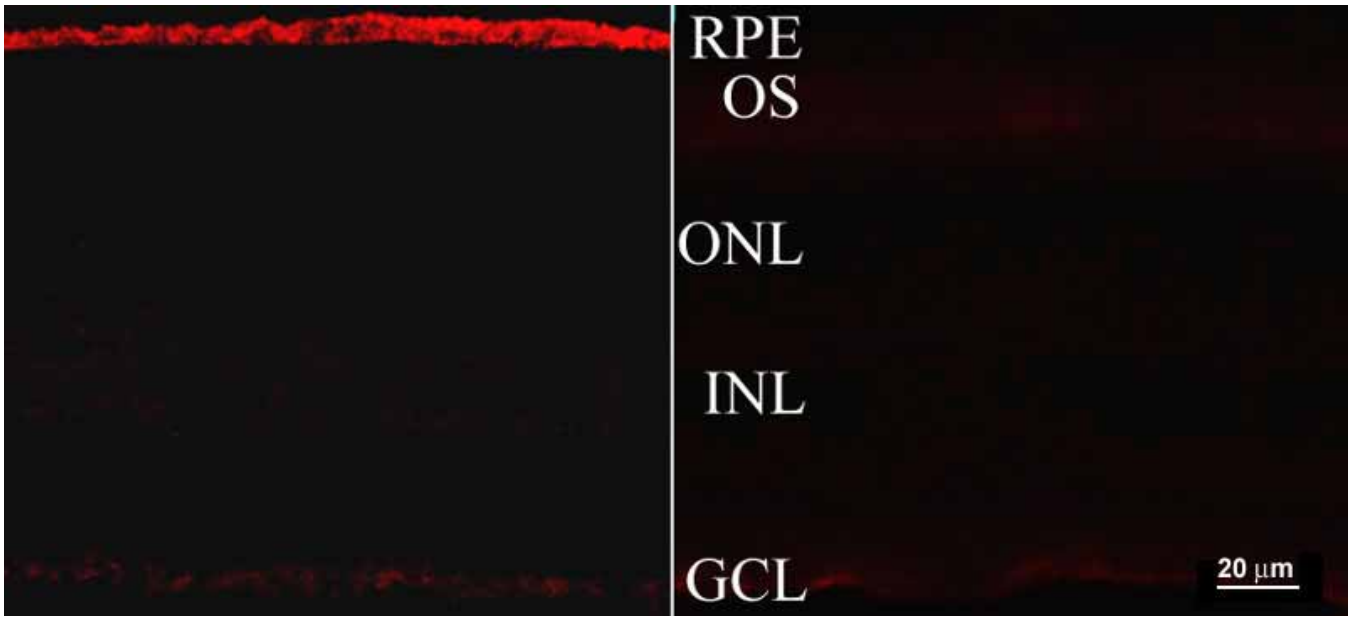

Figure 6. RPE65 expression in retinas of normal C57BL/6J and *rd12* homozygotes by immunostaining. Rpe65 expression was localized primarily in RPE cells of normal retina (left) while no RPE65 was detected in the *rd12* retina (right). The retinal pigment epithelium (RPE), outer segments (OS), outer nuclear layer (ONL), inner nuclear layer (INL), and ganglion cell layer (GCL) are labeled.

lation of retinyl esters relative to normal controls. Compared to C57BL/6J mice, retinal esters in *rd12* homozygotes were approximately 10 fold higher by 5 months of age when the typical retinal white dots first appeared in the fundus of *rd12* homozygotes.

DISCUSSION

With the model reported in this paper, there are now two mouse models for the human disease resulting from mutations in *RPE65*. The first model was created by homologous recombination involving replacement of the first three exons and intervening introns of *Rpe65* by a neomycin resistance cassette [7]. No fundus abnormalities in this *Rpe65* knockout mouse model were reported. This is in contrast to the *rd12* mice, which have small white dots throughout their retinas. These are most easily seen at 6 to 9 months of age. It is not clear that such late stages were examined in the *Rpe65* knockout mouse. In the model we now describe, a naturally occurring homozygous 130 C to T transition creates a premature stop codon, R44X, in exon 3 that is predicted to result in loss of function due to severe truncation of the protein and nonsense mediated mRNA degradation. At least five other nonsense mutations are known among the more than 60 *RPE65* mutations found in retinal dystrophy patients, with over half of all reported mutations predicting premature stop codons due to splice site defects, point mutations, and small rearrangements [26]. The retinas of some of these *Rpe65* lesion patients (RP20) have little white dots [27]. RPE65 loss of function due to the R44X mutation in *rd12* homozygotes was confirmed in our studies by analysis of retinal function, protein expression, and vitamin A metabolism. A complementation test between $Rpe65^{rd12}$ and *Rpe65* knockout was not done; however, phenotypic rescue is seen upon gene replacement therapy (data to be published).

Mice homozygous for *rd12* have small, evenly spaced yellowish white dots throughout their retinas. These small white dots become apparent upon ophthalmoscopic examination by 5 months of age. The clinical phenotype of retinal spots and flecks associated with retinal degeneration in *rd12* homozygotes is similar to human fundus albipunctatus (FA) caused by biochemical defects in the *RDH5* gene encoding 11-*cis* retinol dehydrogenase [28]. The *Rdh5* gene maps to distal mouse Chromosome 10 [29,30], whereas the *rd12* mutation is located on distal Chromosome 3 where the *Rpe65* gene is located. Vitamin A deficiency also can be associated with white dots evenly distributed throughout the fundus and such a phenotype can be difficult to distinguish from FA. However, with vitamin A therapy, spots correlated with the deficient state rapidly disappear [31]. We therefore suggest that the clinical phenotype of the *rd12/rd12* mouse retina further supports the proposed role of RPE65 in disease and in vitamin A metabolism in the visual cycle.

Our biochemical studies of *rd12* homozygotes are consistent with previous findings that RPE65 is required for the conversion of vitamin A to 11-*cis* retinal by the RPE [4]. The ERG phenotype in the *rd12* mouse is similar to that previously reported in RPE65 deficient animal models in which ERG responses were essentially undetectable to all but the brightest stimuli. A recent study investigating the origin of residual function in the RPE65 -/- mouse suggests that a desensitized rod system is responsible for the detectable signals at the highest intensities, even under light adapted conditions [9]. We find no detectable 11-*cis* retinal in the opsin purified

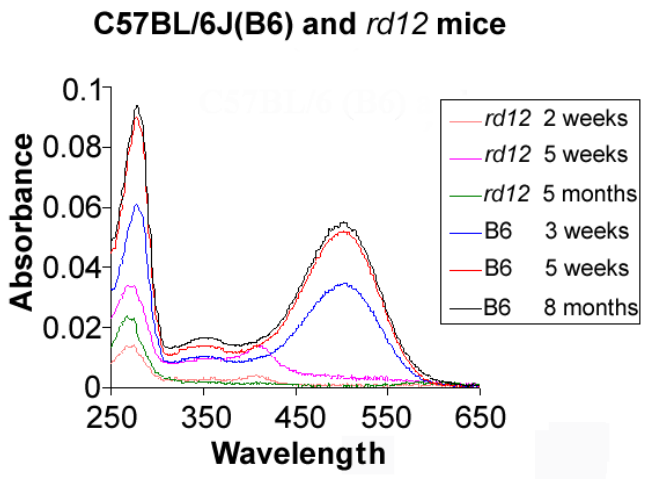

Figure 7. Rhodopsin absorption spectrum in normal C57BL/6J and *rd12* retinas. By 3 weeks of age more than half of the adult level of rhodopsin had been produced in normal mice; by 5 weeks nearly the mature level was reached. In contrast, *rd12* homozygotes exhibited essentially no rhodopsin spectrum at any age (lower 3 curves).

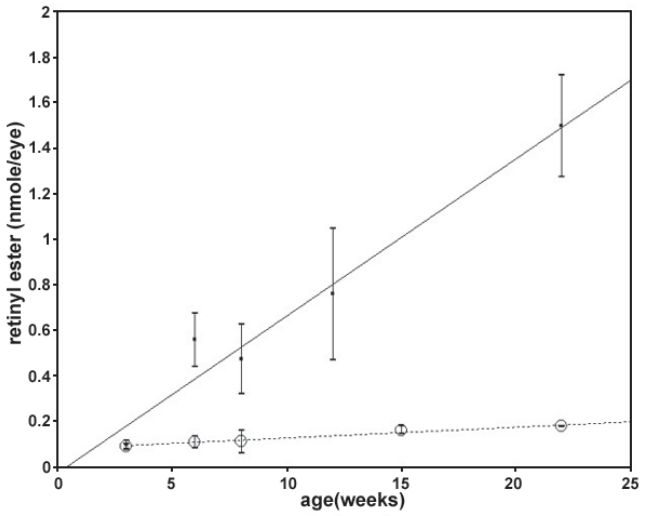

Figure 8. Retinyl esters in normal C57BL/6J and *rd12* homozygote eyes by HPLC analysis. Retinyl ester analysis was done on the eyecups of each of at least 3 mice and averaged. The data points represent means and the error bars represent the standard errors of the mean. Data for *rd12* mice are shown as filled squares. The solid line is the least squares fit of the *rd12* data to a straight line. Data for C57BL/6J are shown as open circles. The dashed line is the least squares fit of the C57BL/6J data to a straight line. Retinyl esters were at similar levels in both *rd12* and C57BL/6J at 3 weeks of age. The retinyl ester content of the C57BL/6J eyes remained stable in the following weeks while the retinyl ester content of the *rd12* mice increased greatly.

from the *rd12* mouse, and a steady accumulation of retinyl esters in the RPE cells with age. In the absence of RPE65, all-*trans* retinyl esters are expected to accumulate in droplets within RPE cells, consistent with a block in 11-*cis* retinal synthesis following esterification of vitamin A to membrane phospholipids before the isomerization reaction. Although the details of the role of RPE65 in the isomerase reaction have not been fully elucidated, recent studies suggest that RPE65 is a retinyl ester binding protein that may function to present all-*trans* retinyl esters to the isomerase [32-34]. The requirement for RPE65 in the synthesis of 11-*cis* retinal has been further substantiated by the finding that addition of recombinant RPE65 to RPE microsomal membranes prepared from *Rpe*65 knockout mice restores retinoid isomerase activity to the preparations [35,36]. Accordingly, adding 11-cis retinal to retinal organ cultures or homogenized retinas from young *rd12* mice leads to formation of rhodopsin (data not shown).

As a result of decreased 11-*cis* retinal synthesis, *rd12* homozygotes do not generate normal levels of visual pigments and have severely depressed dark adapted ERG responses. A similar phenotype is also present in a strain of Swedish Briard dogs carrying a functionally null allele of canine *Rpe*65 [37,38] that are afflicted with progressive retinal dystrophy [39,40]. Affected Briards were recently used in the first successful gene replacement therapy experiments in a large animal model of retinal degeneration [41]. Similar treatment has been attempted in the *rd12* mouse with a significant fraction of the visual function restoration [42], but in the *Rpe65* knockout mouse with limited success [43]. In other studies, administration of oral retinoids to *Rpe65* knockout mice resulted in partial restoration of visual pigment and function [8,44]. The same feeding experiment has not yet been done in our laboratory, but *rd12* mice are available from TJL. The identification of *rd12* as a spontaneously arising mouse model, which has similar *RPE65* mutations to those found in human patients now makes available a powerful new independent model for studying the pathogenesis and progression of LCA. One of the most exciting future uses is likely to involve the study of therapies for LCA and autosomal recessive retinitis pigmentosa in humans.

ACKNOWLEDGEMENTS

We thank The Jackson Laboratory Microchemistry Service for DNA sequencing. These data were generated through the use of GenBank, Celera Discovery System, and Celera Genomics' associated databases. We also thank Dr. T. Michael Redmond (NEI, NIH) for the RPE65 antibody and Denifield W. Player, Dept. of Anatomy and Cell Biology at University of Florida for the EM pictures. This study was supported by National Institutes of Health Grants EY07758, EY11123, EY11996, EY13729, RR01183, and CA34196 and Research to Prevent Blindness, Inc. Parts of this work were presented in abstract form at the annual meeting of The Association for Research in Vision and Ophthalmology, May 2002, Ft. Lauderdale, FL. W. W. Hauswirth has a financial interest in the use of AAV vectors for treating retinal diseases associated with his involvement with Applied Genetic Technologies Corporation (Alachua, FL).

REFERENCES

1. Marlhens F, Bareil C, Griffoin JM, Zrenner E, Amalric P, Eliaou C, Liu SY, Harris E, Redmond TM, Arnaud B, Claustres M, Hamel CP. Mutations in RPE65 cause Leber's congenital amaurosis. Nat Genet 1997; 17:139-41.
2. Morimura H, Fishman GA, Grover SA, Fulton AB, Berson EL, Dryja TP. Mutations in the RPE65 gene in patients with autosomal recessive retinitis pigmentosa or leber congenital amaurosis. Proc Natl Acad Sci U S A 1998; 95:3088-93.
3. Nicoletti A, Wong DJ, Kawase K, Gibson LH, Yang-Feng TL, Richards JE, Thompson DA. Molecular characterization of the human gene encoding an abundant 61 kDa protein specific to the retinal pigment epithelium. Hum Mol Genet 1995; 4:641-9.
4. Thompson DA, Gal A. Genetic defects in vitamin A metabolism of the retinal pigment epithelium. Dev Ophthalmol 2003; 37:141-54.
5. Hamel CP, Jenkins NA, Gilbert DJ, Copeland NG, Redmond TM. The gene for the retinal pigment epithelium-specific protein RPE65 is localized to human 1p31 and mouse 3. Genomics 1994; 20:509-12.
6. Chang B, Hawes NL, Hurd RE, Davisson MT, Nusinowitz S, Heckenlively JR. A point mutation in the Rpe65 gene causes retinal degeneration (rd12) in mice. ARVO Annual Meeting; 2002 May 5-10; Fort Lauderdale (FL).
7. Redmond TM, Yu S, Lee E, Bok D, Hamasaki D, Chen N, Goletz P, Ma JX, Crouch RK, Pfeifer K. Rpe65 is necessary for production of 11-cis-vitamin A in the retinal visual cycle. Nat Genet 1998; 20:344-51.
8. Van Hooser JP, Aleman TS, He YG, Cideciyan AV, Kuksa V, Pittler SJ, Stone EM, Jacobson SG, Palczewski K. Rapid restoration of visual pigment and function with oral retinoid in a mouse model of childhood blindness. Proc Natl Acad Sci U S A 2000; 97:8623-8.
9. Seeliger MW, Grimm C, Stahlberg F, Friedburg C, Jaissle G, Zrenner E, Guo H, Reme CE, Humphries P, Hofmann F, Biel M, Fariss RN, Redmond TM, Wenzel A. New views on RPE65 deficiency: the rod system is the source of vision in a mouse model of Leber congenital amaurosis. Nat Genet 2001; 29:70-4.
10. Fan J, Rohrer B, Moiseyev G, Ma JX, Crouch RK. Isorhodopsin rather than rhodopsin mediates rod function in RPE65 knockout mice. Proc Natl Acad Sci U S A 2003; 100:13662-7.
11. Woodruff ML, Wang Z, Chung HY, Redmond TM, Fain GL, Lem J. Spontaneous activity of opsin apoprotein is a cause of Leber congenital amaurosis. Nat Genet 2003; 35:158-64.
12. Chang B, Heckenlively JR, Hawes NL, Roderick TH. New mouse primary retinal degeneration (rd-3). Genomics 1993; 16:45-9.
13. Heckenlively JR, Chang B, Erway LC, Peng C, Hawes NL, Hageman GS, Roderick TH. Mouse model for Usher syndrome: linkage mapping suggests homology to Usher type I reported at human chromosome 11p15. Proc Natl Acad Sci U S A 1995; 92:11100-4.
14. Chang B, Bronson RT, Hawes NL, Roderick TH, Peng C, Hageman GS, Heckenlively JR. Retinal degeneration in motor neuron degeneration: a mouse model of ceroid lipofuscinosis. Invest Ophthalmol Vis Sci 1994; 35:1071-6.
15. Hawes NL, Chang B, Hageman GS, Nusinowitz S, Nishina PM, Schneider BS, Smith RS, Roderick TH, Davisson MT, Heckenlively JR. Retinal degeneration 6 (rd6): a new mouse model for human retinitis punctata albescens. Invest Ophthalmol Vis Sci 2000; 41:3149-57.
16. Chang B, Hawes NL, Hurd RE, Davisson MT, Nusinowitz S, Heckenlively JR. Retinal degeneration mutants in the mouse.

Vision Res 2002; 42:517-25.
17. Hawes NL, Smith RS, Chang B, Davisson M, Heckenlively JR, John SW. Mouse fundus photography and angiography: a catalogue of normal and mutant phenotypes. Mol Vis 1999; 5:22 .
18. Buffone GJ, Darlington GJ. Isolation of DNA from biological specimens without extraction with phenol. Clin Chem 1985; 31:164-5.
19. Taylor BA, Navin A, Phillips SJ. PCR-amplification of simple sequence repeat variants from pooled DNA samples for rapidly mapping new mutations of the mouse. Genomics 1994; 21:626-32.
20. Lessell S, Kuwabara T. Fine structure of experimental cyanide optic neuropathy. Invest Ophthalmol 1974; 13:748-56.
21. Pang J, Seko Y, Tokoro T. Processes of blue light-induced damage to retinal pigment epithelial cells lacking phagosomes. Jpn J Ophthalmol 1999; 43:103-8.
22. Noorwez SM, Kuksa V, Imanishi Y, Zhu L, Filipek S, Palczewski K, Kaushal S. Pharmacological chaperone-mediated in vivo folding and stabilization of the P23H-opsin mutant associated with autosomal dominant retinitis pigmentosa. J Biol Chem 2003; 278:14442-50. Erratum in: J Biol Chem 2003; 278:21314.
23. Groenendijk GW, De Grip WJ, Daemen FJ. Quantitative determination of retinals with complete retention of their geometric configuration. Biochim Biophys Acta 1980; 617:430-8.
24. Smith WC, Goldsmith TH. Phyletic aspects of the distribution of 3-hydroxyretinal in the class Insecta. J Mol Evol 1990; 30:72-84.
25. Maeda T, Van Hooser JP, Driessen CA, Filipek S, Janssen JJ, Palczewski K. Evaluation of the role of the retinal G protein-coupled receptor (RGR) in the vertebrate retina in vivo. J Neurochem 2003; 85:944-56.
26. Thompson DA, Gal A. Vitamin A metabolism in the retinal pigment epithelium: genes, mutations, and diseases. Prog Retin Eye Res 2003; 22:683-703.
27. Gu SM, Thompson DA, Srikumari CR, Lorenz B, Finckh U, Nicoletti A, Murthy KR, Rathmann M, Kumaramanickavel G, Denton MJ, Gal A. Mutations in RPE65 cause autosomal recessive childhood-onset severe retinal dystrophy. Nat Genet 1997; 17:194-7.
28. Yamamoto H, Simon A, Eriksson U, Harris E, Berson EL, Dryja TP. Mutations in the gene encoding 11-cis retinol dehydrogenase cause delayed dark adaptation and fundus albipunctatus. Nat Genet 1999; 22:188-91.
29. Driessen CA, Winkens HJ, Kuhlmann LD, Janssen BP, van Vugt AH, Deutman AF, Janssen JJ. Cloning and structural analysis of the murine GCN5L1 gene. Gene 1997; 203:27-31.
30. Gamble MV, Shang E, Zott RP, Mertz JR, Wolgemuth DJ, Blaner WS. Biochemical properties, tissue expression, and gene structure of a short chain dehydrogenase/reductase able to catalyze cis-retinol oxidation. J Lipid Res 1999; 40:2279-92.
31. De Laey JJ. Flecked retina disorders. Bull Soc Belge Ophtalmol 1993; 249:11-22.
32. Mata NL, Moghrabi WN, Lee JS, Bui TV, Radu RA, Horwitz J, Travis GH. Rpe65 is a retinyl ester binding protein that presents insoluble substrate to the isomerase in retinal pigment epithelial cells. J Biol Chem 2004; 279:635-43.
33. Jahng WJ, David C, Nesnas N, Nakanishi K, Rando RR. A cleavable affinity biotinylating agent reveals a retinoid binding role for RPE65. Biochemistry 2003; 42:6159-68.
34. Rando RR, Jahng W, David C, Nesnas N, Nakanishi K. Retinoid affinity biotinylation reveals a retinoid binding role for Rpe65. ARVO Annual Meeting; 2003 May 4-9; Fort Lauderdale (FL).
35. Crouch RK, Moiseyev G, Goletz P, Bealle G, Redmond TM, Ma JX. RPE65 is essential but not sufficient for production of 11-cis retinal. Invest Ophthalmol Vision Sci 2001; 42:S655.
36. Crouch RK, Kefalov V, Gartner W, Cornwall MC. Use of retinal analogues for the study of visual pigment function. Methods Enzymol 2002; 343:29-48.
37. Veske A, Nilsson SE, Narfstrom K, Gal A. Retinal dystrophy of Swedish briard/briard-beagle dogs is due to a 4-bp deletion in RPE65. Genomics 1999; 57:57-61.
38. Aguirre GD, Baldwin V, Pearce-Kelling S, Narfstrom K, Ray K, Acland GM. Congenital stationary night blindness in the dog: common mutation in the RPE65 gene indicates founder effect. Mol Vis 1998; 4:23 .
39. Wrigstad A, Narfstrom K, Nilsson SE. Slowly progressive changes of the retina and retinal pigment epithelium in Briard dogs with hereditary retinal dystrophy. A morphological study. Doc Ophthalmol 1994; 87:337-54.
40. Narfstrom K. Retinal dystrophy or 'congenital stationary night blindness' in the Briard dog. Vet Ophthalmol 1999; 2:75-6.
41. Acland GM, Aguirre GD, Ray J, Zhang Q, Aleman TS, Cideciyan AV, Pearce-Kelling SE, Anand V, Zeng Y, Maguire AM, Jacobson SG, Hauswirth WW, Bennett J. Gene therapy restores vision in a canine model of childhood blindness. Nat Genet 2001; 28:92-5.
42. Pang J, Chang B, Heckenlively J, Hawes NL, Nusinowitz S, Noorwez SM, McDowell JH, Timmers AM, Hauswirth WW. Gene therapy restores vision in a natural model of RPE65 leber congenital amaurosis: the rd12 mouse. ARVO Annual Meeting; 2004 April 25-29; Fort Lauderdale (FL).
43. Lai CM, Yu MJ, Brankov M, Barnett NL, Zhou X, Redmond TM, Narfstrom K, Rakoczy PE. Recombinant adeno-associated virus type 2-mediated gene delivery into the Rpe65-/- knockout mouse eye results in limited rescue. Genet Vaccines Ther 2004; 2:3.
44. Van Hooser JP, Liang Y, Maeda T, Kuksa V, Jang GF, He YG, Rieke F, Fong HK, Detwiler PB, Palczewski K. Recovery of visual functions in a mouse model of Leber congenital amaurosis. J Biol Chem 2002; 277:19173-82.

The print version of this article was created on 28 Feb 2005. This reflects all typographical corrections and errata to the article through that date. Details of any changes may be found in the online version of the article.